J Neuropathol Exp Neurol
Vol. 78, No. 6, June 2019, pp. 480–491
doi: 10.1093/jnen/nlz028

ORIGINAL ARTICLE

Enhanced GABAergic Immunoreactivity in Hippocampal Neurons and Astroglia of Multiple Sclerosis Patients

Svenja Kiljan, MSc, Marloes Prins, MSc, Bart M. Baselmans, PhD, John G.J.M. Bol, BASc
Geert J. Schenk, PhD, and Anne-Marie van Dam, PhD

Abstract

Cognitive dysfunction occurs frequently in multiple sclerosis (MS). Research suggests that hippocampal lesions and GABAergic neurotransmitter changes contribute to cognitive dysfunction. In the present study, we aim to determine the cellular changes in GABAergic expression in MS hippocampus related to inflammation and demyelination. To this end, the presence and inflammatory activity of demyelinating lesions was determined by immunohistochemistry in human postmortem hippocampal tissue of 15 MS patients and 9 control subjects. Subsequently, GABAergic cells were visualized using parvalbumin (PV) and glutamate acid decarboxylase 67 (GAD67) markers. Fluorescent colabeling was performed of GAD67 with neuronal nuclei, PV, astrocytic glial fibrillary acidic protein, or vesicular GABA transporter. We observed increased GAD67-positive ($GAD67^+$) neuron and synapse numbers in the CA1 of MS patients with active hippocampal lesions, not due to neurogenesis. The number and size of PV-positive neurons remained unchanged. $GAD67^+$ astrocytes were more numerous in hippocampal white matter than grey matter lesions. Additionally, in MS patients with active hippocampal lesions $GAD67^+$ astrocyte surface area was increased. Disturbed cognition was most prevalent in MS patients with active hippocampal lesions. Summarizing, increased GAD67 immunoreactivity occurs in neurons and astrocytes and relates to hippocampal inflammation and possibly disturbed cognition in MS.

Key Words: Astrocyte, GABA, Glutamate acid decarboxylase, Hippocampus, Interneuron, Multiple sclerosis, Parvalbumin.

INTRODUCTION

Multiple sclerosis (MS) is a chronic inflammatory and demyelinating disease of the central nervous system (CNS), and is the most common disabling neurological disease in young adults (1). Besides the well-known motor and sensory impairments, it has become clear that about half of the MS patients suffer from cognitive dysfunction (2–5). The cause of cognitive impairment in MS is currently unknown, but an increasing number of studies suggest that hippocampal pathology is importantly involved.

The hippocampus plays a key role in cognitive functioning and is involved in various cognitive domains (6), of which memory is the most prominent. Demyelinating lesions within the hippocampus of MS patients have been shown in postmortem tissue (7–10) as well as in vivo using magnetic resonance imaging (MRI) techniques (11, 12). Moreover, hippocampal lesion number was related to visuo-spatial memory functioning in vivo (12). Especially the cornu ammonis 1 (CA1) region of the hippocampus is essential for spatial and nonspatial memory (13, 14). A significant decrease in CA1 volume of the hippocampus of MS patients has been observed and was associated with cognitive dysfunction (15). Finally, neurotransmitter systems are also known to be involved in the interplay of learning and memory processes in the hippocampus (16–20), including γ-aminobutyric acid (GABA) (21, 22). GABA is the major inhibitory neurotransmitter in the mammalian CNS and is synthesized from glutamate by the enzyme glutamic acid decarboxylase (GAD). Two isoforms of GAD, that is, GAD65 and GAD67, have been identified. Within the hippocampus, most GABAergic neurons contain relatively high levels of GAD67, which is present in neuronal terminals and cell bodies (23). GAD67 is known to have trophic effects after neuronal injury and in development but also in the adult brain shapes neuronal circuits during neurogenesis (24, 25). In addition, GABAergic neurons are well known for their abilities to synchronize neuronal networks, which is important for cognitive processing (26). In particular, functional parvalbumin (PV) neurons, a subtype of GABAergic neurons, in the hippocampus seem important for certain hippocampus-dependent memory tasks in rodents (27, 28).

In addition to neurons, astrocytes play an active role in regulating neurotransmission processes, for example, by the uptake of glutamate, its conversion into glutamine and/or GABA, and the release of glutamate and GABA into the

From the Department of Anatomy and Neurosciences, Amsterdam UMC, Vrije Universiteit Amsterdam, Amsterdam Neuroscience, Amsterdam, The Netherlands (SK, MP, BMB, JGJMB, GJS, AMvD).
Send correspondence to: Anne-Marie van Dam, PhD, Department of Anatomy and Neurosciences, Amsterdam UMC, VU University Medical Center, De Boelelaan 1108, 1081 HZ Amsterdam, The Netherlands; E-mail: amw.vandam@vumc.nl
Present address: Bart M. Baselmans, Department of Biological Psychology, VU University, Amsterdam, The Netherlands.
Svenja Kiljan and Marloes Prins shared first authorship.
Funding for this study was received from the Dutch MS Research Society for their financial support (grant 14-358e MS).
The authors have no duality or conflicts of interest to declare.

extracellular space (29–31). Human astrocytes were shown to express GAD67 (30), and recently it was shown that an increase in astrocytic GABA release in the hippocampus interfered with neurotransmission resulting in poor memory performance in a mouse model of Alzheimer disease (32).

Although overall increased hippocampal mRNA GAD67 levels have been reported in MS (7), cell specific contributions, the relation with hallmarks of MS pathology (i.e. demyelination and inflammation) and whether these changes relate to cognitive features of patients are unclear so far. Therefore, the present study investigated neuronal, synaptic and astrocytic immunoreactivity for GAD67, and neuronal PV immunoreactivity in hippocampal MS (chronic) active and inactive lesions, normal appearing white matter (NAWM) and normal appearing grey matter (NAGM) compared with non-neurological controls.

MATERIALS AND METHODS

Human Subjects

Informed consent was given by the donors for brain autopsy and use of brain tissue for research purposes. Use of tissue in combination with the clinical information for scientific research was in compliance with the local ethical and legal guidelines.

Postmortem human hippocampal tissue was obtained from the Netherlands Brain Bank ([NBB] Amsterdam, The Netherlands) or from the Department of Pathology (VU University Medical Center in Amsterdam, The Netherlands). Formalin-fixed, paraffin-embedded hippocampal tissue sections were included from 15 clinically diagnosed and neuropathologically verified MS patients (age range: 43–76 years) and 9 control subjects (age range: 50–92 years) without neurological or psychiatric disease. Subjective cognitive dysfunction of a number of these MS patients has been identified, as it was reported in their medical record by their general practitioner or neurologist. Four out of 5 (80%) MS patients with active hippocampal lesions had a history of cognitive deficits, also specifically reporting memory problems. Two out of 6 (33%) MS patients with chronic inactive hippocampal lesions had a history of cognitive deficits and 1 out of 4 (25%) MS patients without hippocampal lesions reported cognitive deficits. Finally, none of the control subjects reported cognitive problems. All relevant clinicopathological data of the MS patients and nonneurological control subjects are provided in Table 1.

Categorization of MS Hippocampi Based on Lesion Status

For immunohistochemical analysis, we have divided our study subjects into 4 categories: Control subjects, MS patients without hippocampal lesions, MS patients with only inactive hippocampal lesions and MS patients with active hippocampal lesions. Categorization of MS hippocampi was based on: (i) myelin basic protein (MBP) immunoreactivity to visualize (de)myelination and identify the presence of lesions, and (ii) in case of demyelination, MHC-II immunoreactivity to determine the inflammatory status of the lesions (inactive or active). Both white matter (WM) and grey matter (GM) regions within the human hippocampus were evaluated which included: The alveus, stratum lacunosum, and the CA1, CA2, and CA3 including the stratum oriens, stratum pyramidalis, and stratum radiatum, respectively.

Three types of demyelination patterns were observed throughout the hippocampus: Pure WM lesions (WML), pure GM lesions (GML) and mixed lesions (i.e. if the same lesion comprised both hippocampal GM and WM; Fig. 1A, F). In case of a mixed lesion, the GM part of the lesion was considered a GML and the WM part was considered a WML. The inflammatory activity status of demyelinated lesions was determined by the presence of major histocompatibility class II-positive (MHC-II$^+$) monocytes/macrophages or microglia in the border or center of a lesion (Fig. 1B, G). Active, chronic active and inactive WML were defined as described previously (33, 34), in which active lesions show foamy monocytes/macrophages in the center of lesions (Fig. 1C), chronic active lesions show foamy monocytes/macrophages at the border of lesions (Fig. 1D), while inactive lesions are almost devoid of activated immune cells but do show ramified microglia (Fig. 1H, I) (33–35). GML were considered active or chronic active when MHC-II$^+$ foamy macrophages were present within the neighboring demyelinated WM part of the lesion in case of a mixed lesion or by the presence of MHC-II$^+$ microglia in a pure GML (Fig. 1E). Inactive GML present with few MHC-II$^+$ microglia (Fig. 1J). The category of MS patients referred to in the remainder of the manuscript as having active lesions include hippocampi with active or chronic active lesions.

Immunohistochemical Detection of MBP, MHC-II, PV and GAD67

After rapid autopsy (mean postmortem delay [PMD]: 7.5 hours), tissue blocks were fixed in 4% formalin for 30 days and embedded in paraffin. Of 29 paraffin-embedded tissue blocks, 5-μm sections were cut and mounted on positively charged glass slides (Menzel-Glaser SuperFrost plus, Braunschweig, Germany), and dried overnight at 37°C. Upon use, sections were heated in a stove for 30 minutes at 56°C, before they were deparaffinized in xylene, and rehydrated through a series of 100%, 96%, and 70% ethanol and distilled water. For subsequent antigen retrieval, sections were rinsed in 0.01 M citrate buffer (pH 6.0) or in 0.01 M Tris buffer (pH 9.0) containing 1 mM EDTA (Tris-EDTA) and subsequently heated in a steamer for 30 minutes at 90–99°C in the same buffers. After antigen retrieval, the sections were allowed to regain room temperature (RT), rinsed in Tris-buffered saline (TBS), and incubated for 20 minutes in TBS containing 0.3% H_2O_2 and 0.1% sodiumazide. After rinsing with TBS, nonspecific binding sites were blocked with 5% nonfat dried milk (Campina) in TBS containing 0.5% Triton (TBS-T; blocking solution) for 30 minutes at RT. Subsequently, sections were incubated overnight at 4°C with the following primary antibodies: MBP, MHC-II, PV, or glutamic acid decarboxylase 67 (GAD67; see Table 2 for details on primary antibodies), diluted in blocking solution. The next day, sections were washed in TBS and incubated for 2 hours at RT in corresponding biotinylated IgGs in blocking solution (1:400; Jackson Immunoresearch Laboratories, Westgrove, PA; see Table 2 for details on secondary

TABLE 1. Clinicopathological Data of MS Patients and Control Subjects

Case	Gender	Age	PMD (h)	DD	MS Type	Demyelination (Lesion Type)	Cognitively Impaired	COD
MS								
1	M	43	8:30	17	SP	Yes (active)	Yes	Pneumonia
2	F	66	6:00	23	SP	Yes (active)	Yes	Unknown
3	F	60	10:40	7	PP	Yes (active)	Yes	Euthanasia*
4	M	54	8:15	12	PP	Yes (active)	Yes	Euthanasia*
5	F	50	7:35	17	SP	Yes (active)	Unknown	Euthanasia*
6	F	62	6:45	25	Unknown	Yes (inactive)	Unknown	Unknown
7	M	63	7:05	28	SP	Yes (inactive)	Yes	Cardiac arrest after rupture of abdominal aorta
8	M	49	8:00	26	PP	Yes (inactive)	Unknown	Pneumonia by MS
9	M	66	7:30	26	PP	Yes (inactive)	Yes	Ileus
10	M	61	9:15	31	SP	Yes (inactive)	Unknown	Euthanasia*
11	F	57	8:40	27	Unknown	Yes (inactive)	Unknown	Respiratory insufficiency by (uro)sepsis
12	F	76	9:45	20	PP	No	Unknown	Unknown
13	M	50	9:30	24	PP	No	Unknown	Unknown
14	M	51	11:00	20	Unknown	No	Yes	Unknown
15	M	56	9:50	14	PP	No	Unknown	Cachexia and exhaustion by end stage MS
Control								
1	M	84	7:05				No	Exacerbation of COPD
2	M	56	9:15				Unknown	Myocardial infarction
3	F	62	7:55				No	Euthanasia*
4	F	92	7:00				No	Acute death, probably pulmonary emboly
5	F	50	4:10				No	Metastasized large cell bronchocarcinoma
6	F	62	7:20				Unknown	Metastases
7	M	82	5:10				Unknown	Pneumonia/cardiovascular accidents
8	M	78	Unknown				Unknown	Cardiac arrest after rupture of abdominal aorta
9	F	84	6:55				No	Myelo dysplasia

PMD, postmortem delay; DD, disease duration; COD, cause of death; SP, secondary progressive; PP, primary progressive.
*All subjects that underwent euthanasia were mentally competent to make such a decision.

antibodies), followed by horseradish peroxide (HRP)-labeled avidin-biotin complex ([ABC] 1:400; Vector Laboratories, Burlingame, CA) in TBS for 1 hour at RT. To detect GAD67 immunoreactivity, an amplification step was included at this stage, and thus sections were subsequently rinsed with TBS and incubated in biotinylated tyramide (1:800, kindly provided by Dr. Inga Huitinga, Netherlands Institute for Neuroscience, Amsterdam) and 0.01% peroxide in TBS-T for 30 minutes, followed by rinsing with TBS and another incubation with ABC (1:800) in TBS-T for 1 hour. Detection of all antigens was visualized using 3, 3-diaminobenzidine ([DAB] Sigma, St. Louis, MO) as a chromogen and counterstaining was performed with hematoxylin. After dehydration in graded ethanol solutions, the sections were cleared in xylene and coverslipped in Entellan (Merck, Darmstadt, Germany). Negative controls were performed by omitting the primary antibody, resulting in no immunohistochemical signal (data not shown).

Immunohistochemical Double Labeling of GAD67 and Doublecortin

A light microscopical double labeling was performed to determine colocalization between neurogenesis marker doublecortin (DCX) and GAD67-positive ($GAD67^+$) in MS patients with active hippocampal lesions. The section pretreatment was performed as described above, including deparaffinization, antigen retrieval and blocking. Primary antibodies to GAD67 and DCX (Table 2) were added to the sections simultaneously in blocking solution and incubated overnight at 4°C. The next day, sections were washed in TBS and incubated for 2 hours at RT in biotinylated goat anti guinea pig IgGs (1:400; Vector) in blocking solution, followed by ABC incubation (1:400) in TBS for 1 hour at RT and DCX was visualized using DAB as a chromogen. Then sections were incubated with ImmPRESS anti rabbit (Vector) for 30 minutes, followed by washes in phosphate buffered saline and for visualization of GAD67, the sections were incubated with liquid permanent red (LPR 1:107; DAKO, Amsterdam, The Netherlands) as a chromogen for 30 minutes. Finally, the sections were counterstained with hematoxylin and air-dried overnight. The next day sections were dipped in xylene and coverslipped in Entellan.

Immunofluorescent Double Labeling of GAD67 with NeuN, PV, vGAT or GFAP

A fluorescent double labeling was performed to determine colocalization of GAD67 with glial fibrillary acidic protein (GFAP) in astrocytes and of GAD67 with PV in

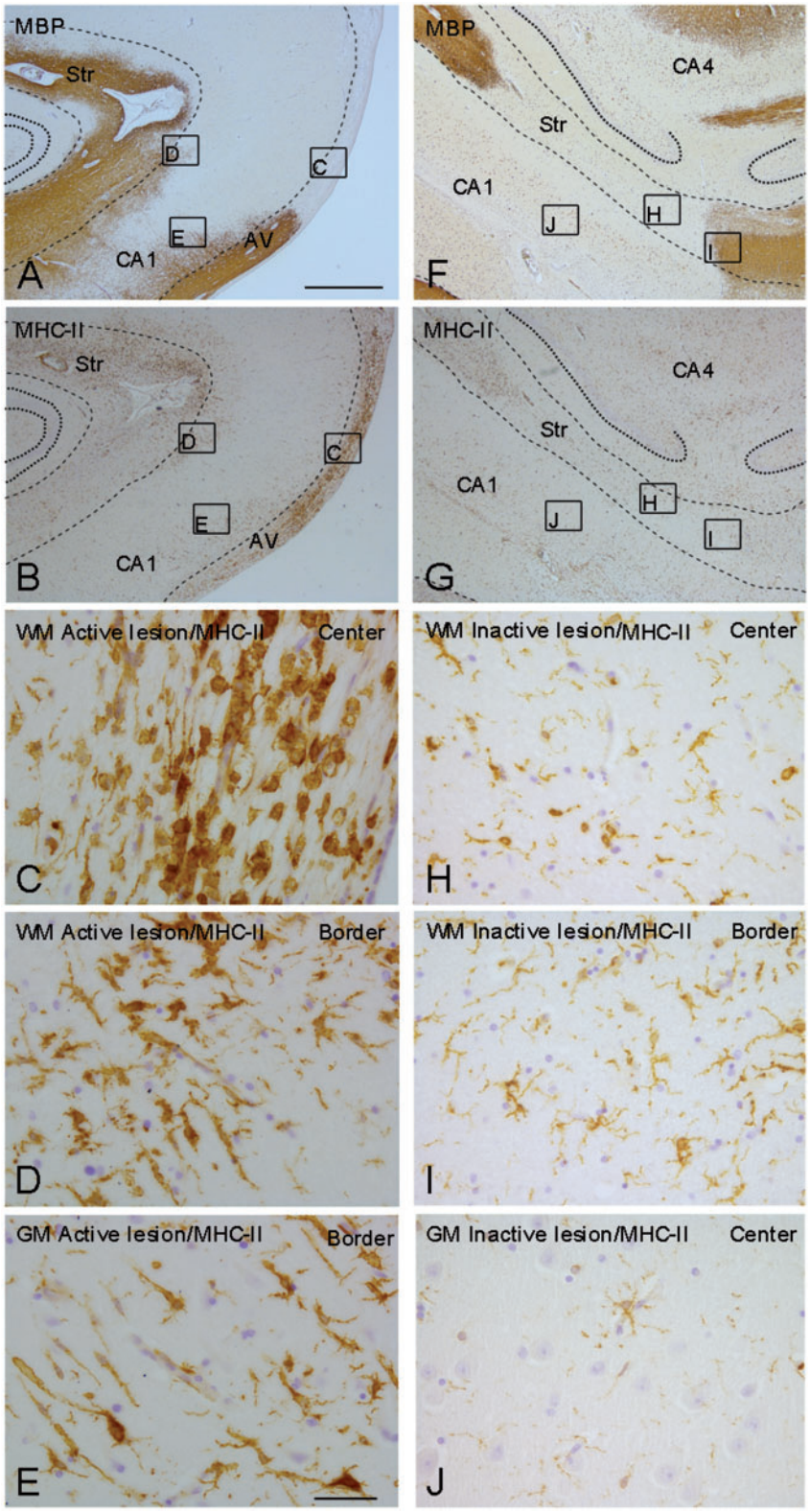

FIGURE 1. Histopathological features of active and inactive hippocampal MS lesions. MS lesions were recognized by the loss of myelin basic protein (MBP) immunoreactivity in hippocampal white matter (WM) and/or grey matter (GM) areas **(A, F)**. Active and inactive lesions were distinguished based on the presence, density and morphology of MHC-II$^+$ monocytes/macrophages in the center or at the border of a demyelinated hippocampal lesion **(B, G)**. An active WML characterized by activated amoeboid-shaped MHC-II$^+$ cells in the center of a demyelinated lesion **(C)**. An active WM lesion (WML) characterized by activated MHC-II$^+$

TABLE 2. Primary and Secondary Antibodies Used for Antigen Labeling

Antigen	Antigen Retrieval	Species	Final Dilution	Source Primary Antibody, Article Number	Secondary Antibody	Source Secondary Antibody, Article Number
Human MBP	Tris-EDTA	Mouse	1:100	Boehringer, 1118099	Biotinylated donkey anti mouse IgG	Jackson, 715-065-151
Human MHC-II	Citrate	Mouse	1:100	Gift, Clone LN3	Biotinylated donkey anti mouse IgG	Jackson, 715-065-151
Human PV	Tris-EDTA	Mouse	1:300	Sigma, P3088	Biotinylated donkey anti mouse IgG	Jackson, 715-065-151
Human GAD67	Tris-EDTA	Rabbit	1:400	Anaspec, 53501	Biotinylated goat anti rabbit IgG	Jackson, 111-065-144
Pig GFAP	Tris-EDTA	Mouse	1:300	Sigma, G3893	Alexa Fluor-594 labeled donkey anti mouse IgG	Molecular Probes, R37115
Murine DCX	Tris-EDTA	Guinea pig	1:3000	Chemicon, AB5910	Biotinylated goat anti guinea IgG	Vector, BA7000
Mouse NeuN	Tris-EDTA	Mouse	1:400	Chemicon, MAB377	Biotinylated donkey anti mouse IgG	Jackson, 715-065-151
Rat vGAT	Tris-EDTA	Chicken	1:100	Synaptic Systems, 131 006	Alexa Fluor-488 labeled donkey anti chicken IgG	Jackson, 703-545-155

interneurons or with neuronal neuronal nuclei (NeuN) or with vesicular synaptic GABA transporter vesicular GABA transporter (vGAT). The deparaffinization process, pretreatment and blocking procedures were as described in a previous section. Then, antibodies to GAD67 and GFAP (Table 2) were diluted in blocking solution and simultaneously incubated overnight at 4°C. The next day, after rinsing in TBS, the sections were incubated with Alexa Fluor-594 labeled donkey anti mouse IgGs (1:400, Molecular Probes, Eugene, OR) and with biotinylated donkey anti rabbit IgGs (1:400, Jackson Immunoresearch Laboratories) diluted in blocking solution for 2 hours at RT. Subsequently, the sections were rinsed in TBS and incubated with ABC (1:800) in TBS for 1 hour at RT and finally followed by incubation with biotinylated tyramide (1:800, gift Dr. Inga Huitinga, NIN, Amsterdam) in TBS + 0.005% H_2O_2 for 20 minutes, washed in TBS and incubated with streptavidin-labeled Alexa Fluor-488 (1:400, Molecular Probes). Fluorescent images were obtained with a confocal microscope (Leica Microsystems, Wetzlar, Germany) at 63× magnification.

For double labeling of GAD67 with PV or NeuN, sections were incubated overnight at 4°C with the PV or NeuN antibody in blocking solution. The next day, after washes with TBS, sections were incubated with biotinylated donkey anti mouse IgGs (1:400, Jackson Immunoresearch Laboratories), diluted in blocking solution for 2 hours at RT, followed by rinses in TBS and incubation with ABC (1:800) in blocking solutions for 1 hour at RT for PV staining and with streptavidin with conjugated HRP (1:800, Jackson Immunoresearch Laboratories) for 2 hours at RT for NeuN staining. Finally, sections were rinsed in TBS and incubated with Alexa Fluor-488-labeled tyramide for PV staining while incubated with Alexa Fluor-594-labeled tyramide for NeuN staining (both 1:800, Perkin Elmer, Waltham, MA) diluted in TBS + 0.005% H_2O_2 for 10 minutes at RT. Afterwards the sections were heated in a steamer for 40 minutes at 90–99°C in Tris-EDTA to remove any of the bound antibodies, but leaving the precipitate of the fluorescently labeled tyramide at PV or NeuN antigen binding sites. For double labeling of GAD67 with vGAT, sections were incubated overnight at 4°C with vGAT and the next day after washes with TBS incubated with Alexa Fluor-488 labeled donkey anti chicken IgG (1:200, Jackson Immunoresearch Laboratories) for 2 hours at RT. Subsequently, GAD67 antibody (1:800) diluted in blocking solution was added to the sections overnight at 4°C for all 3 double stainings (GAD67 with vGAT, NeuN, or PV). After washes in TBS, the sections were incubated with biotinylated donkey anti rabbit IgGs (1:400) diluted in blocking solution, for 2 hours at RT. Subsequently, sections were rinsed with TBS and incubated with ABC (1:800) in blocking solution for 1 hour at RT and followed by rinses in TBS and incubation with biotinylated tyramide (1:800) in TBS + 0.005% H_2O_2 for 10 minutes at RT. Then, after rinsing, sections were incubated with Alexa Fluor-594-labeled streptavidin (1:400; Molecular Probes) in case of double labeling with GFAP and vGAT or with Alexa Fluor-488-labeled streptavidin (1:400; Molecular Probes) in case of double labeling with PV and NeuN, for 2 hours at RT. Finally, after a last step of rinsing in TBS, fluorescently stained sections were coverslipped with DABCO (Sigma). Fluorescent images were obtained using a confocal microscope (Leica Microsystems) at 63× magnification.

FIGURE 1. Continued
cells at the border of the demyelinated lesion **(D)**. An active purely GM lesion (GML) characterized by activated MHC-II$^+$ cells at the border of the demyelinated lesion **(E)**. An inactive WML characterized by less densely packed MHC-II$^+$ cells with a ramified morphology, in the center and border of the demyelinated lesions **(H, I)**. An inactive GML characterized by few MHC-II$^+$ cells with a ramified morphology in center **(J)** or border (not shown), of the demyelinated lesion. The square frames marked with [C], [D], and [E] in panels **A** and **B** refer to the high-magnification images in panels **C**, **D**, and **E**, respectively. The square frames marked with [H], [I], and [J] in panels **F** and **G** refer to the high-magnification images in panels **H**, **I**, and **J**, respectively. The dashed lines indicate the border between hippocampal WM and GM in panels **A**, **B**, **F**, and **G**. AV, alveus; Str, stratum. Scale bar in **A** = 1 mm and also applies to **B**, **F, G**; scale bar in **E** = 50 μm and also applies to **C, D, H–J.**

Semiquantitative Analysis of PV$^+$ and GAD67$^+$ Interneurons

PV-positive (PV$^+$) and GAD67$^+$ neurons were counted in the CA1 region, since this region is critically involved in spatial and nonspatial memory (13, 14). Furthermore, in hippocampal tissue used in this study, the CA1 exhibited the highest frequency of lesions, compared with other CA regions, which is in line with previous studies (15, 30). Within the CA1 area, the stratum oriens, stratum pyramidalis and stratum radiatum were evaluated all together for each control subject and MS patient. Unbiased manual counting of the GAD67$^+$ and PV$^+$ neurons was performed on stitched digital images of the entire CA1 region of the hippocampus present in one section per staining. The counting area of the CA1 in control subjects and MS patients without hippocampal lesions was 1.40–4.80 mm^2 (absolute PV$^+$ number counted: Range: 1–38, median: 12; for GAD67$^+$ range: 2–64, median: 25.50). In MS patients with active or inactive hippocampal lesions the counting area was 0.90–4.20 mm^2 for CA1 NAGM (absolute PV$^+$ number counted: Range: 3–44, median: 19; absolute GAD67$^+$ number counted: Range: 6–237, median: 78) and the counting area of CA1 lesions was 0.2–3.3 mm^2 (absolute PV$^+$ number counted: Range: 1–53, median: 8; absolute GAD67$^+$ number counted: Range: 0–127, median: 67.50). GAD67$^+$ and PV$^+$ neurons were only counted when a nucleus was clearly visible and when they showed a neuronal morphology. Final results were expressed as cell number per mm^2. All images were acquired using an Olympus-VANOX-T microscope (Tokyo, Japan) at 10× magnification. Cell counting and area determination were performed using CelÎF Olympus Soft Imaging Software (Tokyo, Japan). Additionally, the size of PV$^+$ interneurons was measured at 20× magnification of all counted PV$^+$ neurons. Images were acquired and analyzed using a Leica Ctr 5000 microscope and appurtenant software (Leica Microsystems). Subsequently, ImageJ was used to determine the cell surface area in μm^2 as a measure of PV$^+$ neuron size. All neuron surface measurements were averaged per subject.

Semiquantitative Analysis of the GAD67$^+$ Synapses

GAD67 also stains inhibitory synapses. These were quantified in the CA1 region of the hippocampus as the number of GAD67$^+$ synapses per mm^2. For imaging, Stereo Investigator software (MBF Bioscience, Williston, VT) was used that was connected to a Leica DMR microscope (Leica Microsystems). The CA1 region, including the stratum oriens, stratum pyramidalis, and stratum radiatum, was manually outlined at 2.5× magnification. The outlined region of interest (ROI) was the same as for the quantification of GAD67$^+$ and PV neuron densities. Subsequently, automatic random systematic sampling was performed at 100× magnification using an oil lens, resulting in ∼20 images within the ROI of every section. ImageJ (version 1.52a, https://imagej.net/Fiji) was used to segment synapses from the images, GAD67$^+$ structures were only considered as synapses when small punctae had a size between 0.25 and 3 μm^2 (see review [36]) (37). Blood vessels, cell bodies, and nuclei were manually outlined in every image and subtracted from the image area before the synaptic density per mm^2 was calculated.

Semiquantitative Analysis of GAD67$^+$ Astrocytes

GAD67$^+$ astrocytes were counted either in NAGM of hippocampal (CA1, CA2, and CA3) regions in the stratum pyramidalis and in NAWM regions including the stratum lacunosum and the alveus of control subjects and MS patients without hippocampal lesions. The same WM and GM areas were analyzed in MS patients with active or inactive hippocampal lesions, but just within lesions. Semiquantification of GAD67$^+$ astrocytes was performed by manually counting the number of GAD67$^+$ cells with a clearly visible cell nucleus and astrocytic morphology within ROIs. In each section, 4 different ROIs were identified. Two ROIs comprised only hippocampal WM, while 2 other ROIs were positioned on hippocampal GM. Counting areas were varying from 0.1 to 0.4 mm^2. Final results were expressed as cell number per mm^2. Images were acquired and analyzed as described above.

Semiquantitative Analysis of the GAD67$^+$ Astrocyte Surface Area

In addition to the number of GAD67$^+$ astrocytes in the hippocampus, we measured the surface area of astrocytic GAD67 immunoreactivity in hippocampal WM, including the stratum lacunosum and the alveus. WML in MS patients with inactive or active lesions was compared with WM of MS patients without lesions and of control subjects. The level of GAD67 immunoreactivity in astrocytes was not determined in hippocampal GM, since GM barely showed GAD67$^+$ astrocytes. Thus, 2 ROIs were positioned at the WM regions of the hippocampus, that is, one at the alveus and one at the stratum lacunosum, corresponding to the WM ROI's used for the GAD67$^+$ astrocyte count. In each ROI 2 images were taken at 20× magnification. All images were acquired and analyzed using a Leica Ctr 5000 microscope and appurtenant software (Leica Microsystems). GAD67 immunoreactivity was measured above a fixed threshold applied to all images to distinguish specific staining from background using Nuance spectral imaging software (Nuance version 3.0.2, Caliper Kife Sciences, Inc, a Perkin Elmer Company, Hopkinton, MA). The results were calculated as the percentage of area containing GAD67 immunoreactivity over the total area analyzed.

Statistical Analysis

Statistical analyses were carried out with SPSS package version 20.0 (Statistical Product and Service Solutions, Chicago, IL). Normal distribution of the data was tested using the Shapiro-Wilk procedure. When data were normally distributed, differences between control subjects, MS patients without hippocampal lesions, MS patients with active hippocampal lesions or MS patients with inactive hippocampal lesions were compared using one-way ANOVA, followed by Tukey's post hoc analysis. When data were not normally distributed, a Kruskal-Wallis test was performed followed by

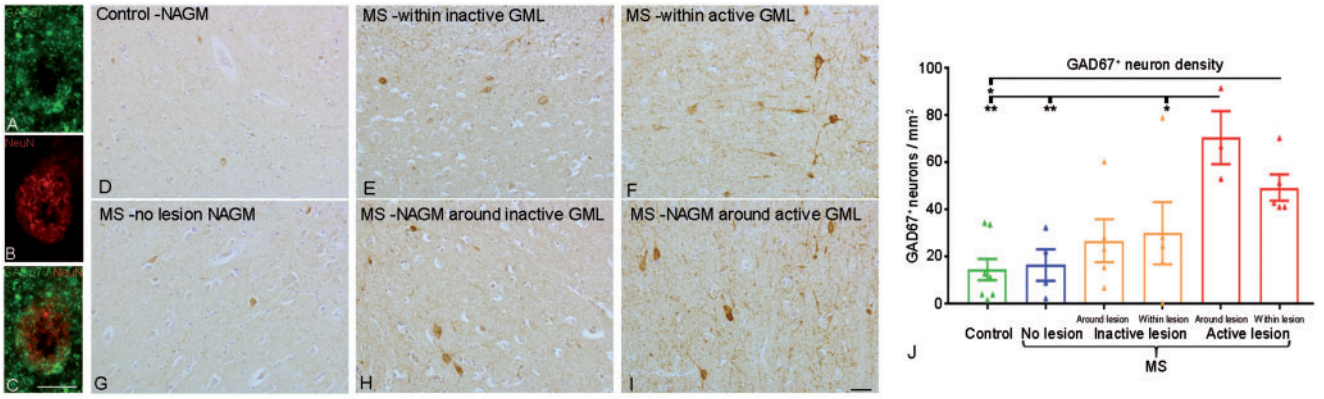

FIGURE 2. Semiquantitative analysis of GAD67$^+$ neurons within hippocampal CA1. GAD67$^+$ neurons were also NeuN$^+$ **(A–C)**. GAD67$^+$ neuronal immunoreactivity was present in the CA1 of control subjects **(D)**, in inactive **(E)** or active **(F)** MS lesions in the CA1 of MS patients, in the CA1 of MS patients without lesions **(G)** and in CA1 normal appearing grey matter (NAGM) surrounding MS inactive **(H)** or active **(I)** MS lesions. Semiquantitative analysis of GAD67$^+$ neuron density showed that this was not different between control subjects and MS patients without hippocampal lesions **(J)**. A significant increase in the density of GAD67$^+$ neurons was found within lesions and surrounding NAGM of MS patients with active hippocampal lesions compared with hippocampal NAGM of control subjects **(J)**. GAD67$^+$ neuron density was significantly higher in NAGM surrounding lesions in MS patients with active hippocampal lesions compared with MS patients with inactive hippocampal lesions or without hippocampal lesions **(J)**. Data in graphs represent individual patient data-points and mean + SEM. Scale bar in **C** = 10 μm and applies to **A, B**; scale bar in **I** = 50 μm and also applies to **D–H**. *$p < 0.05$, **$p < 0.01$.

a Mann-Whitney *U* post hoc analysis. Differences in GAD67$^+$ astrocytes cell counts within subject WM and GM were analyzed for control subjects, MS patients without and with hippocampal demyelination using the Wilcoxon Signed Rank Test. GAD67$^+$ astrocyte surface area was not normally distributed and was therefore subjected to a square root transformation. Following this transformation, normality of distribution was confirmed, followed by one-way ANOVA and Tukey's post hoc analysis. Although information on the cognitive status of MS patients and controls was scarce, all GAD67 scores were compared between cognitively intact and cognitively disturbed individuals using the Student's *t*-test. In addition, all GAD67 scores were correlated with the cognitive status of patients and controls, age, gender, PMD and disease duration, using a Pearson's correlation coefficient when data were normally distributed and a Spearman's correlation coefficient when data were not normally distributed. p values < 0.050 were considered significant.

RESULTS

Lesion Characterization

As indicated in Figure 1, areas of hippocampal demyelination were identified by loss of MBP immunoreactivity in GM and WM areas of the hippocampus. No demyelination was observed in the 9 control subjects (not shown). Of the 15 MS patients, 4 patients did not show demyelination in the hippocampal tissue block obtained. The other 11 MS patients showed demyelinated hippocampal areas, which were subsequently examined for the presence of MHC-II$^+$ cells to determine the lesion inflammatory activity status (Fig. 1). Of these, 5 patients had lesions that were classified as active or chronic active lesions. Finally, the remaining 6 MS patients were classified as having inactive lesions. Per patient, the immunohistochemical semiquantification was performed on active or inactive lesions and the NAGM around the lesions.

Semiquantitative Analysis of PV$^+$ and GAD67$^+$ Interneurons

Double-labeling experiments showed GAD67$^+$ neurons were also immunopositive for NeuN, indicating that GAD67 indeed labels inhibitory neurons (Fig. 2A–C). An increase in GAD67$^+$ neuron density was observed within lesions in the CA1 of MS patients with active hippocampal lesions and in surrounding NAGM compared with the CA1 of control subjects (ANOVA, $F = 5.526$, $p = 0.002$; Tukey HSD, $p = 0.032$; Tukey HSD, $p = 0.002$, respectively, Fig. 2D–I). Moreover, in this group of MS patients the number of GAD67$^+$ neurons in the NAGM surrounding CA1 lesions was also significantly higher when compared with the CA1 of MS patients without hippocampal lesions and to NAGM surrounding lesions in the CA1 of MS patients that only have inactive hippocampal lesions (ANOVA, $F = 5.526$; $p = 0.002$; Tukey HSD, $p = 0.009$ and $p = 0.037$, respectively; Fig. 2J). To identify whether the observed increase in GAD67 neuron density was possibly due to neurogenesis, a colabeling of DCX and GAD67$^+$ was performed. A very limited amount of DCX$^+$ cells was found and they did not overlap with GAD67$^+$ neurons (data not shown).

PV$^+$ neurons were also GAD67$^+$ (Fig. 3A–C), confirming their identity as a subpopulation of GABAergic neurons. The density of PV$^+$ neurons in the hippocampal CA1 region did not differ between control subjects and MS patients irrespective of hippocampal demyelination and inflammation being present (ANOVA; $F = 0.535$; $p = 0.750$; Fig. 3D–J). Similarly, the size of PV$^+$ neurons was not different between groups (ANOVA; $F = 0.246$; $p = 0.938$; Fig. 3K). The number of PV$^+$ and GAD67$^+$ neurons did not correlate with age, gender, PMD, and disease duration of the patients.

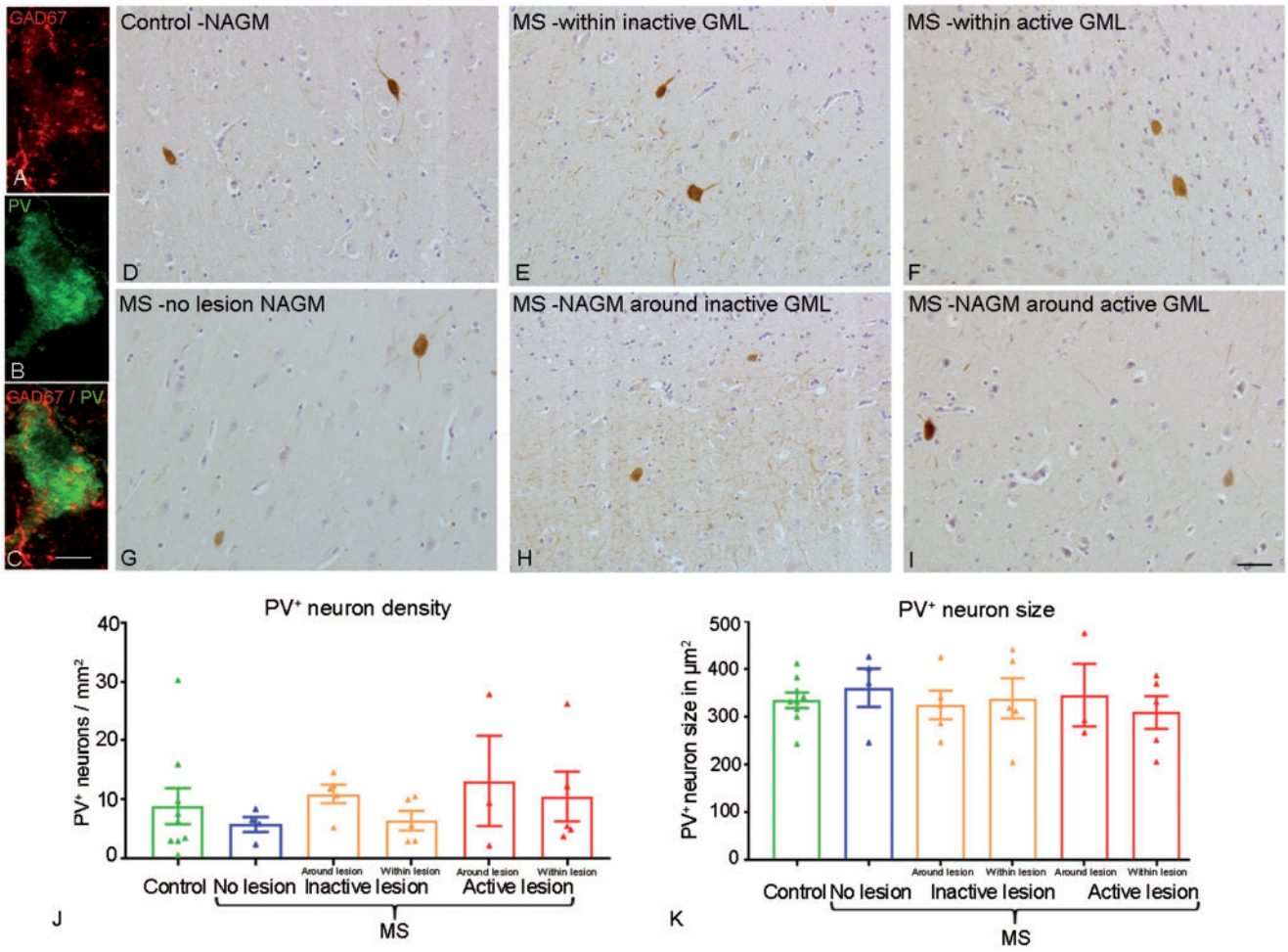

FIGURE 3. Semiquantitative analysis of PV^+ neurons within hippocampal CA1. PV^+ neurons were also $GAD67^+$ **(A–C)**. The PV^+ neuron density and size was not different between control subjects **(D)** and MS patients without hippocampal lesions **(G)**, MS patients with inactive lesions **(E, H)** and MS patients with active lesions **(F, I)**. The PV^+ neuron density was quantified **(J)**. The PV^+ neuron size was quantified **(K)**. Data in graphs represent individual patient data-points and means + SEM. Scale bar in **C** = 10 µm and also applies to **A, B**; scale bar in **I** = 50 µm and also applies to **D–H.**

Semiquantitative Analysis of $GAD67^+$ Synapses

$GAD67^+$ punctae colocalized with vGAT, indicating that these punctae are inhibitory presynapses (Fig. 4A–C). $GAD67^+$ inhibitory synaptic terminal density was quantified in the CA1 region of the hippocampus (Fig. 4D, E). A trend towards a significant difference in synapse count between groups was found (ANOVA, $F = 2.537$, $p = 0.056$). An increase in density was observed in the CA1 of MS patients with hippocampal inflammation within lesions and surrounding NAGM compared with control subjects, MS patients without hippocampal demyelination and MS patients with inactive hippocampal lesions (Fig. 4F).

Semiquantitative Analysis of $GAD67^+$ Astrocytes

We confirmed the astrocyte identity of the $GAD67^+$ cells with astrocytic morphology based on a consistent overlap in immunoreactivity of GAD67 and the astrocyte marker GFAP (Fig. 5A–C). We observed the presence of GAD67 immunoreactivity in cells with an astrocytic morphology in all subjects (Fig. 5D–K). No significant differences were found in $GAD67^+$ astrocyte density in hippocampal WM or GM between MS patients and control subjects (Kruskal-Wallis, $p = 0.210$ and $p = 0.450$, respectively; Fig. 5L). However, there were clearly more $GAD67^+$ astrocytes in hippocampal WML than in GML of MS patients with active hippocampal lesions and in MS patients with inactive hippocampal lesions (Wilcoxon Signed Rank test, $p = 0.040$; Wilcoxon Signed Rank test, $p = 0.030$, respectively; Fig. 5L).

Moreover, analysis of $GAD67^+$ astrocyte surface area showed a significant increase in MS patients with active hippocampal lesions compared with control subjects, MS patients without hippocampal lesions and MS patients with inactive lesions (ANOVA; F11.118; $p < 0.001$; Tukey HSD; $p < 0.001$; $p = 0.002$ and $p = 0.010$, respectively; Fig. 5M). The surface area of $GAD67^+$ astrocytes in WML did not correlate with age, gender, PMD, and disease duration of the patients.

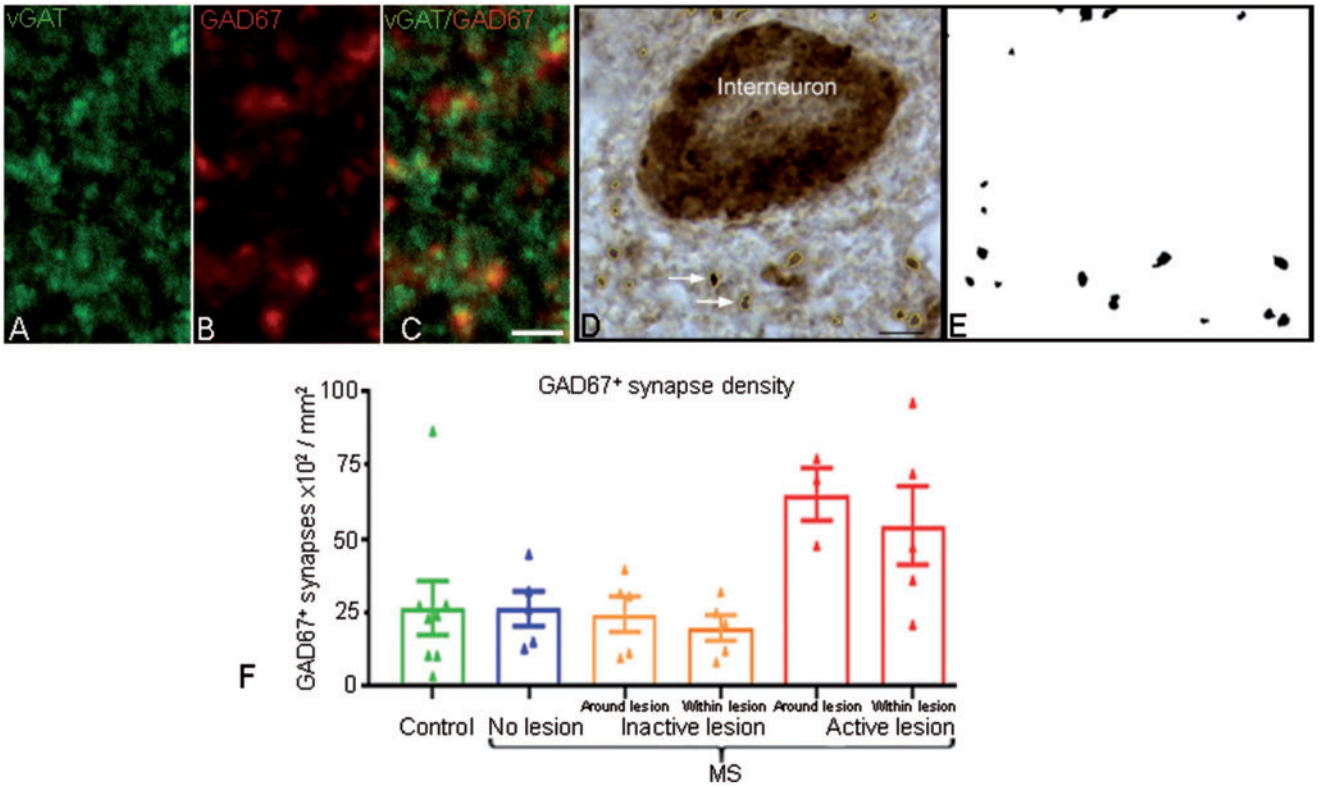

FIGURE 4. Semiquantitative analysis of GAD67$^+$ inhibitory synapses within hippocampal CA1. Double-labeling experiments showed that GAD67$^+$ punctae also expressed vGAT **(A–C)**. GAD67$^+$ inhibitory synapses were outlined (yellow). Arrows show representative GAD67$^+$ synapses **(D)**. A binary image of the outlined synapses from panel **D** was used for synapse quantification **(E)**. A slight increase in synapse density in hippocampal CA1 was observed in MS patients with active lesions compared with control subjects, MS patients without lesions, MS patients with inactive lesions **(F)**; data in graphs represent individual patient data-points and mean + SEM. Scale bar in **C** = 3 μm and also applies to **A, B**; scale bar in **D** = 5μm.

DISCUSSION

The present study is the first to describe cell type specific (i.e. neuronal and astrocytic) alterations in GABAergic expression patterns in MS hippocampus compared with control subjects. We also show that inflammation rather than demyelination relates to alterations in GAD67$^+$ levels, since the number of GAD67$^+$ neurons is significantly increased specifically in the CA1 of MS patients with active hippocampal lesions. Interestingly, the number of PV$^+$ neurons remains unchanged in MS hippocampi compared with control hippocampi. In addition, we find GAD67$^+$ astrocytes to be significantly more numerous in hippocampal WML than GML of MS patients and that the GAD67 astrocyte surface area is significantly increased in MS patients with active hippocampal WML. Interestingly, this relates positively to cognitive disturbance in MS patients.

The increased number of GAD67$^+$ hippocampal neurons and elevated GAD67$^+$ astrocyte surface area are in line with a previous study that documented increased GAD67 mRNA levels in demyelinated MS hippocampi (7), of which we now identified the cell types able to produce GABA in MS hippocampal lesions. Importantly, our data from active versus inactive MS lesions suggest that inflammation, as determined by MHC-II expression, result in enhanced GAD67 immunoreactivity as shown in active lesions, but clearly reduced when inflammation extinguishes as shown in inactive lesions. Moreover, it suggests that inflammation rather than demyelination, being present in both lesion types, may underlie the increase in GAD67 levels in the hippocampus. However, observations regarding GAD67 levels in the MS hippocampus are in contrast to observations in the motor cortex of MS patients where a decrease in GAD67 mRNA was observed (38). Whether this difference in hippocampal versus cortical expression of GAD67 mRNA is due to intrinsic differences within these brain regions, the immunological activity in the tissue or the contribution of astrocytic GAD67 mRNA in the hippocampus remains to be determined. The observed increase in GAD67$^+$ neuron number is not due to neurogenesis since we did not observe a cellular colabeling of GAD67 and DCX, a marker for neurogenesis. We thus conclude that this increase is the result of induced elevation of detectable levels of GAD67$^+$ in pre-existing neurons. Moreover, this could also explain our observation of slightly elevated synaptic density in hippocampi of MS patients with active lesions, a result similar to the GAD67$^+$ neuron count. Overall, our data indicate that inflammation may modulate GAD67$^+$ levels in hippocampal interneurons and their inhibitory synapses. This may have consequences for GABA levels in the hippocampus

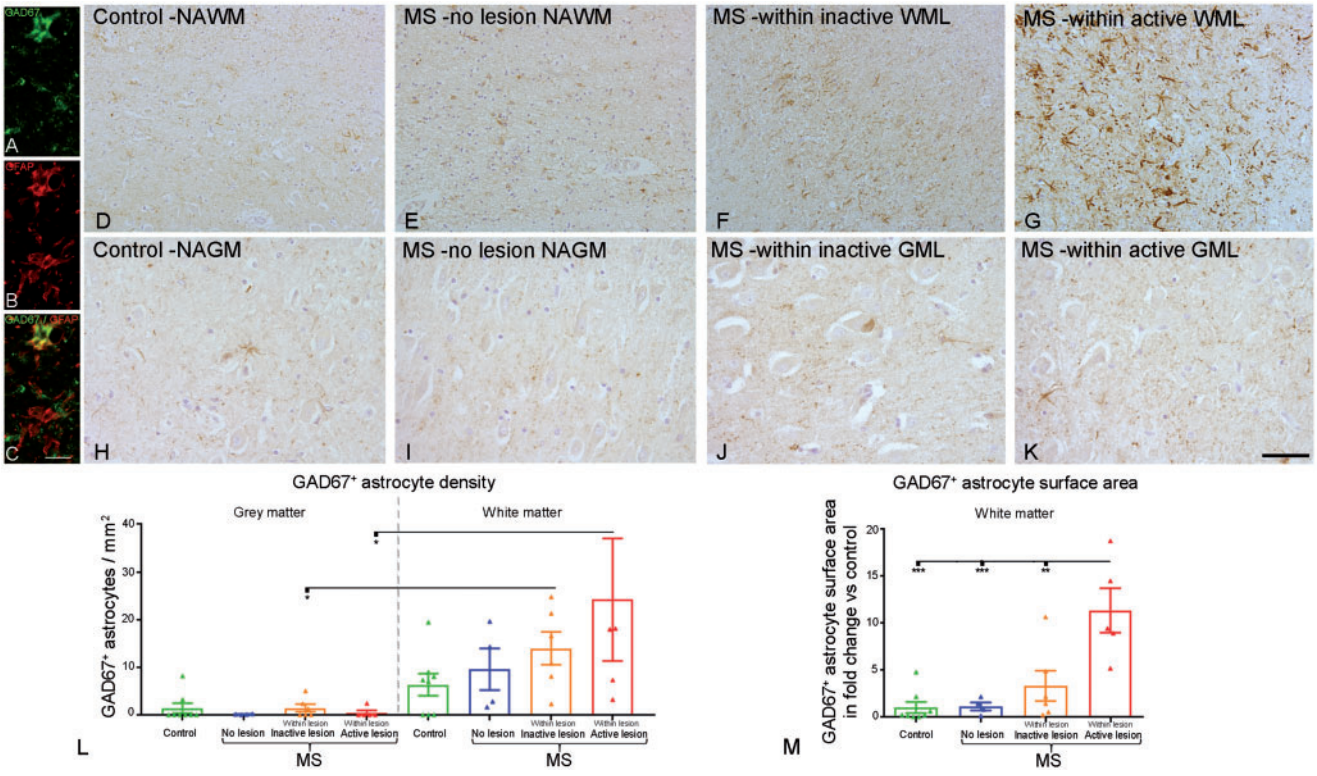

FIGURE 5. Semiquantitative analysis of GAD67$^+$ astrocytes within hippocampal GM and WM. Colabeling showed that GAD67$^+$ cells with astrocytic morphology also expressed GFAP **(A–C)**. No differences in GAD67$^+$ astrocyte density were found between control subjects, MS patients without hippocampal lesions, MS patients with inactive hippocampal lesions, and MS patients with active hippocampal lesions in hippocampal WM (**D–G**) or in GM **(H–K)**. However, GAD67$^+$ astrocyte density in WML **(F, G)** was higher than in GML **(J, K)**, in MS patients with either inactive or active hippocampal lesions **(L)**. The surface area of GAD67$^+$ astrocytes was quantified in hippocampal WM. Hippocampal GAD67$^+$ astrocyte surface area was significantly larger in hippocampal WML of MS patients with active hippocampal lesions compared with MS patients with inactive hippocampal lesions, MS patients without hippocampal lesions and to control subjects **(M)**. Data in graphs represent individual patient datapoints and mean + SEM. Scale bar in **C** = 3 μm and also applies to **A, B**; scale bar in **K** = 50 μm and also applies to **D–J**. *$p < 0.05$, **$p = 0.01$, ***$p < 0.01$.

and consequently an increase in GABA could attenuate excitatory activity and/or toxicity.

Although less PV mRNA was observed in the motor cortex of MS patients compared with control subjects (38), we established that the number of PV$^+$ neurons remained unchanged in hippocampal MS lesions compared with control subjects. In addition, a decrease in PV$^+$ neurites was reported in the motor cortex of patients (38). This suggests that the number of PV expressing neurons in the hippocampus may not be altered, as we observed, but instead the number or complexity of their neuronal processes may be reduced. In line with this, it was reported in an animal model of MS that inflammation modifies dendritic integrity and synapse functioning, and induces synapse loss preceding loss of neurons (39). In neuropsychiatric diseases, such as schizophrenia and depression, loss of (PV$^+$) interneurons and disruption of GABAergic circuits has been described (40, 41). Although degeneration of interneurons likely causes cognitive deficits, disruption of GABAergic circuits may also be caused by altered functioning of interneurons related to synaptic GABAergic neurotransmission rather than degeneration of these cells (42).

Immune cells are known to produce inflammatory cytokines and growth factors, for example, brain-derived neurotrophic factor (BDNF) and interleukin (IL)-1β. Several studies have shown that via the secretion of cytokines and growth factors immune cells are able to affect excitatory and inhibitory neurotransmission. For example, cerebrospinal fluid-derived IL-1β from MS patients with MRI detectable inflammatory brain lesions can inhibit GABAergic neurotransmission in mouse brain slices (43). It has also been shown that IL-1β can induce synaptic hyperexcitability (44) and glutamate excitotoxicity (45, 46). Alternatively, BDNF can promote the expression of GAD67 in primary hippocampal neurons (47). In line with this, transgenic mice with a decreased level of somatic GAD67 showed a reduced neuronal inhibitory efficacy and an altered neuronal excitation and inhibition balance (48). Such changes in the environment of, for example, the hippocampus may interfere with the balance of neuronal excitation and inhibition, which may be of clinical relevance. A tight balance between excitatory and inhibitory inputs within neuronal microcircuits has been hypothesized to be relevant for efficient information processing and cognitive functioning (49).

We observed that changes in the hippocampal GAD67 expression were not solely of neuronal nature since astrocytes also showed altered GAD67 immunoreactivity. Although the number of $GAD67^+$ astrocytes was not changed in MS hippocampal lesions versus control subjects, we did observe significantly more $GAD67^+$ astrocytes in WML than in GML of MS patients with active or inactive hippocampal lesions. This may be due to inflammation having been present in inactive lesions or still being present in active WML, which is generally more pronounced in those WML than in active or inactive GML (reviewed in [50]; Fig. 1B, G).

In contrast to $GAD67^+$ astrocyte number, $GAD67^+$ astrocyte surface area was clearly increased in MS active hippocampal WML compared with inactive WML, to nonlesion WM and to control subject WM. Previous studies indicate that GABA secretion by astrocytes can in a paracrine way have an anti-inflammatory effect on astrocytes and surrounding microglia (30). Thus, the increase in GAD67 in astrocytes solely in lesions with ongoing inflammation may point towards an anti-inflammatory role of astrocytes in the WML.

The proportion of MS patients reporting cognitive deficits was higher in patients with inflamed hippocampal lesions compared with MS patients without hippocampal lesions or with chronic inactive lesions. Notably, patients with active hippocampal lesions also showed increased GAD67 immunoreactivity in astrocytes and neurons. Previous research in a model of Alzheimer disease found that increased astrocytic GABA release contributed to impaired memory performance (32). Whether similar mechanisms may also occur in MS is unknown. Further studies are therefore warranted to perform more extensively neuropsychological testing in MS patients to determine disturbances in various cognitive domains, including memory function. This could be related to either in vivo magnetic resonance spectroscopy or positron emission tomography for GABA (47, 51), or neuronal and astrocytic GABA immunoreactivity at postmortem to determine the role of GABA in those processes.

Overall, we conclude that GAD67 immunoreactivity is increased in neurons and astrocytes in and around hippocampal lesions in MS, especially in hippocampi with active lesions. The increased GAD67 immunoreactivity likely depends more on hippocampal inflammation rather than demyelination. We propose that increased GAD67 may result in enhanced GABA levels, which may hamper hippocampal function and, in the end, could possibly contribute to disturbed cognition in MS.

ACKNOWLEDGMENTS

Prof. Dr. P. van der Valk and Prof. Dr. S. Amor (VUmc, Dept. Pathology) are thanked for their help defining the lesion types in the MS hippocampal material.

REFERENCES

1. Noseworthy JH, Lucchinetti C, Rodriguez M, et al. Multiple sclerosis. N Engl J Med 2000;343:938–52
2. Benedict RH, Zivadinov R. Risk factors for and management of cognitive dysfunction in multiple sclerosis. Nat Rev Neurol 2011;7:332–42
3. Chiaravalloti ND, DeLuca J. Cognitive impairment in multiple sclerosis. Lancet Neurol 2008;7:1139–51
4. Hulst HE, Schoonheim MM, Roosendaal SD, et al. Functional adaptive changes within the hippocampal memory system of patients with multiple sclerosis. Hum Brain Mapp 2012;33:2268–80
5. Rocca MA, Amato MP, De Stefano N, et al. Clinical and imaging assessment of cognitive dysfunction in multiple sclerosis. Lancet Neurol 2015; 14:302–17
6. Strange BA, Witter MP, Lein ES, et al. Functional organization of the hippocampal longitudinal axis. Nat Rev Neurosci 2014;15:655–69
7. Dutta R, Chang A, Doud MK, et al. Demyelination causes synaptic alterations in hippocampi from multiple sclerosis patients. Ann Neurol 2011; 69:445–54
8. Geurts JJ, Bo L, Roosendaal SD, et al. Extensive hippocampal demyelination in multiple sclerosis. J Neuropathol Exp Neurol 2007;66: 819–27
9. Papadopoulos D, Dukes S, Patel R, et al. Substantial archaeocortical atrophy and neuronal loss in multiple sclerosis. Brain Pathol 2009;19: 238–53
10. Vercellino M, Masera S, Lorenzatti M, et al. Demyelination, inflammation, and neurodegeneration in multiple sclerosis deep gray matter. J Neuropathol Exp Neurol 2009;68:489–502
11. Roosendaal SD, Geurts JJ, Vrenken H, et al. Regional DTI differences in multiple sclerosis patients. Neuroimage 2009;44:1397–403
12. Roosendaal SD, Moraal B, Vrenken H, et al. In vivo MR imaging of hippocampal lesions in multiple sclerosis. J Magn Reson Imaging 2008;27: 726–31
13. Rampon C, Tang YP, Goodhouse J, et al. Enrichment induces structural changes and recovery from nonspatial memory deficits in CA1 NMDAR1-knockout mice. Nat Neurosci 2000;3:238–44
14. Tsien JZ, Huerta PT, Tonegawa S. The essential role of hippocampal CA1 NMDA receptor-dependent synaptic plasticity in spatial memory. Cell 1996;87:1327–38
15. Sicotte NL, Kern KC, Giesser BS, et al. Regional hippocampal atrophy in multiple sclerosis. Brain 2008;131:1134–41
16. Stelzer A, Simon G, Kovacs G, et al. Synaptic disinhibition during maintenance of long-term potentiation in the CA1 hippocampal subfield. Proc Natl Acad Sci U S A 1994;91:3058–62
17. Hasselmo ME. The role of acetylcholine in learning and memory. Curr Opin Neurobiol 2006;16:710–5
18. Deiana S, Platt B, Riedel G. The cholinergic system and spatial learning. Behav Brain Res 2011;221:389–411
19. Davies CH, Starkey SJ, Pozza MF, et al. GABA autoreceptors regulate the induction of LTP. Nature 1991;349:609–11
20. Bashir ZI, Bortolotto ZA, Davies CH, et al. Induction of LTP in the hippocampus needs synaptic activation of glutamate metabotropic receptors. Nature 1993;363:347–50
21. Andrews-Zwilling Y, Gillespie AK, Kravitz AV, et al. Hilar GABAergic interneuron activity controls spatial learning and memory retrieval. PLoS One 2012;7:e40555
22. Murray AJ, Sauer JF, Riedel G, et al. Parvalbumin-positive CA1 interneurons are required for spatial working but not for reference memory. Nat Neurosci 2011;14:297–9
23. Houser CR, Esclapez M. Localization of mRNAs encoding two forms of glutamic acid decarboxylase in the rat hippocampal formation. Hippocampus 1994;4:530–45
24. Pinal CS, Tobin AJ. Uniqueness and redundancy in GABA production. Perspect Dev Neurobiol 1998;5:109–18
25. Akerman CJ, Cline HT. Refining the roles of GABAergic signaling during neural circuit formation. Trends Neurosci 2007;30:382–9
26. Uhhaas PJ, Singer W. Neural synchrony in brain disorders: Relevance for cognitive dysfunctions and pathophysiology. Neuron 2006;52: 155–68
27. Aika Y, Ren JQ, Kosaka K, et al. Quantitative analysis of GABA-like-immunoreactive and parvalbumin-containing neurons in the CA1 region of the rat hippocampus using a stereological method, the disector. Exp Brain Res 1994;99:267–76
28. Fuchs EC, Zivkovic AR, Cunningham MO, et al. Recruitment of parvalbumin-positive interneurons determines hippocampal function and associated behavior. Neuron 2007;53:591–604
29. Lee M, McGeer EG, McGeer PL. Mechanisms of GABA release from human astrocytes. Glia 2011;59:1600–11
30. Lee M, Schwab C, McGeer PL. Astrocytes are GABAergic cells that modulate microglial activity. Glia 2011;59:152–65

31. Parpura V, Basarsky TA, Liu F, et al. Glutamate-mediated astrocyte-neuron signalling. Nature 1994;369:744–7
32. Jo S, Yarishkin O, Hwang YJ, et al. GABA from reactive astrocytes impairs memory in mouse models of Alzheimer's disease. Nat Med 2014;20:886–96
33. Bo L, Mork S, Kong PA, et al. Detection of MHC class II-antigens on macrophages and microglia, but not on astrocytes and endothelia in active multiple sclerosis lesions. J Neuroimmunol 1994;51: 135–46
34. Trapp BD, Peterson J, Ransohoff RM, et al. Axonal transection in the lesions of multiple sclerosis. N Engl J Med 1998;338:278–85
35. van der Valk P, De Groot CJ. Staging of multiple sclerosis (MS) lesions: Pathology of the time frame of MS. Neuropathol Appl Neurobiol 2000; 26:2–10
36. O'Rourke NA, Weiler NC, Micheva KD, et al. Deep molecular diversity of mammalian synapses: Why it matters and how to measure it. Nat Rev Neurosci 2012;13:365–79
37. Rutten BP, Wirths O, Van de Berg WD, et al. No alterations of hippocampal neuronal number and synaptic bouton number in a transgenic mouse model expressing the beta-cleaved C-terminal APP fragment. Neurobiol Dis 2003;12:110–20
38. Dutta R, McDonough J, Yin X, et al. Mitochondrial dysfunction as a cause of axonal degeneration in multiple sclerosis patients. Ann Neurol 2006;59:478–89
39. Mandolesi G, Gentile A, Musella A, et al. Synaptopathy connects inflammation and neurodegeneration in multiple sclerosis. Nat Rev Neurol 2015;11:711–24
40. Grace AA. Dysregulation of the dopamine system in the pathophysiology of schizophrenia and depression. Nat Rev Neurosci 2016;17:524–32
41. Benes FM, Berretta S. GABAergic interneurons: Implications for understanding schizophrenia and bipolar disorder. Neuropsychopharmacology 2001;25:1–27
42. Marin O. Interneuron dysfunction in psychiatric disorders. Nat Rev Neurosci 2012;13:107–20
43. Rossi S, Studer V, Motta C, et al. Inflammation inhibits GABA transmission in multiple sclerosis. Mult Scler 2012;18:1633–5
44. Rossi S, Furlan R, De Chiara V, et al. Interleukin-1beta causes synaptic hyperexcitability in multiple sclerosis. Ann Neurol 2012;71:76–83
45. Mandolesi G, Musella A, Gentile A, et al. Interleukin-1beta alters glutamate transmission at purkinje cell synapses in a mouse model of multiple sclerosis. J Neurosci 2013;33:12105–21
46. Nistico R, Mango D, Mandolesi G, et al. Inflammation subverts hippocampal synaptic plasticity in experimental multiple sclerosis. PLoS One 2013;8:e54666
47. Freeman L, Garcia-Lorenzo D, Bottin L, et al. The neuronal component of gray matter damage in multiple sclerosis: A [(11) C]flumazenil positron emission tomography study. Ann Neurol 2015;78:554–67
48. Lazarus MS, Krishnan K, Huang ZJ. GAD67 deficiency in parvalbumin interneurons produces deficits in inhibitory transmission and network disinhibition in mouse prefrontal cortex. Cereb Cortex 2015;25:1290–6
49. Deneve S, Machens CK. Efficient codes and balanced networks. Nat Neurosci 2016;19:375–82
50. Prins M, Schul E, Geurts J, et al. Pathological differences between white and grey matter multiple sclerosis lesions. Ann N Y Acad Sci 2015;1351: 99–113
51. Cawley N, Solanky BS, Muhlert N, et al. Reduced gamma-aminobutyric acid concentration is associated with physical disability in progressive multiple sclerosis. Brain 2015;138:2584–95